Functional MRI Detection of Bilateral Cortical Reorganization in the Rodent Brain Following Peripheral Nerve Deafferentation

Galit Pelled, **Kai-Hsiang Chuang**, **Stephen J Dodd**, and **Alan P Koretsky**[*]
Laboratory of Functional and Molecular Imaging, National Institute of Neurological Disorders and Stroke, National Institutes of Health, Bethesda, MD

Abstract

Evidence is emerging for significant inter-hemispheric cortical plasticity in humans, opening important questions about the significance and mechanism for this long range plasticity. In this work, peripheral nerve deafferentation was performed on both the rat forepaw and hindpaw and cortical reorganization was assessed using functional MRI (fMRI). Sensory stimulation of the forepaw or the hindpaw in rats that experienced only partial denervation resulted in activation in only the appropriate, contralateral, primary somatosensory cortex (SI). However, 2-3 weeks following complete denervation of the rats' forepaw or hindpaw, stimulation of the intact paw resulted in fMRI activation of ipsilateral as well as contralateral SI. To address whether inter-cortical communication is required for this cortical reorganization, the healthy hindpaw SI representation was stereotaxically lesioned in rats which had the other hindpaw denervated. No fMRI activation was detected in the ipsilateral SI cortex after lesioning of the contralateral cortex. These results indicate that extensive inter-hemispheric cortical-cortical reorganization can occur in the rodent brain after peripheral nerve deafferentation and that cortical–cortical connections play a role in mediating this inter-hemispheric cortical reorganization.

Keywords

functional MRI; somatosensory cortex; plasticity; peripheral nerves; denervation; rat

Introduction

A major emphasis by numerous groups for several years has been to understand cortical reorganization that occurs after peripheral nerve injury. It has been demonstrated that removal of the sensory input from a specific region of the adult neocortex, such as severing a major nerve can lead to a large reorganization of cortical topography within the deprived area (Borsook, 1998; Chen, 2002; Merzenich, 1983; Metzler and Marks, 1979; Wall and Cusick, 1984). Many studies have demonstrated how adjacent cortical regions within the same hemisphere or peripheral areas proximate to the non-innervated region can occupy the deprived somatosensory cortical region. Although this form of cortical plasticity is well documented across several sensory systems and in several species, the understanding of the underlying mechanisms remains an active area of research. There are several mechanisms that contribute to these intrahemispheric changes, such as reorganization of the thalamus (Verley and Onnen,

1981), changes in the strength of the thalamus projections to the primary somatosensory cortex (SI) (Kaas, 1999; Krupa, 1999; Stojic, 1998; Verney, 1982) and changes in SI intra-cortical connections themselves, such as strengthening or sprouting of pre-existing connections (Darian-Smith and Gilbert, 1994; Merzenich, 1983; Wall and Cusick, 1984).

There is growing evidence that, in addition to cortical plasticity between neighboring regions in the same hemisphere, there can be long range plasticity occurring between cortical hemispheres. Most of the evidence comes from studies of direct cortical damage such as stroke or cortical lesions in human and animal models (Abo, 2001; Caramia, 1996; Dijkhuizen, 2001; Kim, 2003; Kim, 2005; Luke, 2004; Reinecke, 2003; Rema and Ebner, 2003). In these cases, peripheral inputs normally evoking responses in the region damaged cause functional responses in the opposite and normally inappropriate hemisphere. In addition to direct damage of the cortex causing inter-cortical plasticity, peripheral nerve deafferentation has also all been shown to elicit bilateral cortical responses in humans (Werhahn, 2003). Furthermore, temporary deafferentation of the digits in the flying fox (Calford and Tweedale, 1990; Clarey, 1996), monkey (Clarey, 1996) and rat (Shin, 1997) showed immediate expansions of the receptive fields of adjacent body parts both in the contralateral SI and the ipsilateral SI. Inspired by the results from human and animal studies, the present work aimed to test the extent of long distance cortical-cortical reorganization in the rodent brain after peripheral nerve injury.

The vast majority of animal work studying cortical plasticity has been performed using electrophysiology. Multi-unit electrophysiological recording can be obtained with excellent temporal and spatial resolution. However, a major drawback is that one can only obtain information from one or a few localized areas and from a limited number of cells. Therefore, many aspects of cortical reorganization, such as global network rearrangements and changes in region to region functional connectivity have been difficult to assess. Functional MRI (fMRI) using blood oxygenation level dependent (BOLD) contrast of rodents now enable spatial resolution of less than a couple of hundred microns and temporal resolution on the order of 100 ms (Keilholz, 2004; Kim, 2000; Kim and Ugurbil, 1997; Mandeville, 1998; Silva and Koretsky, 2002) making MRI an increasingly useful tool for studying plasticity in small animal models.

The goal of the present work was to investigate the consequences of peripheral nerve injury on cortical reorganization in the rat brain using fMRI. In particular, intercortical reorganization and the involvement of cortico-cortical pathways on inter-hemispheric reorganization were studied. The peripheral nerves in the rat forepaw or hindpaw were denervated, and high-field fMRI measurements at 11.7 T were made to assess the degree of cortical reorganization.

Materials and Methods

Animal model

All experiments were performed in compliance with guidelines set by the National Institutes of Neurological Disorders and Stroke ACUC. A total of 47 Sprague-Dawley rats were used for the following studies:

Nerve deafferentation procedure—Previously it was demonstrated that consumption of soy-containing diets preoperatively and postoperatively suppressed development of mechanical and heat allodynia, as well as hyperalgesia in rodents (Shir, 2001). Therefore, rats were fed with RMH-1000 soy diet (PMI Feeds) a week prior to the surgery and continuing throughout the study. Sprague-Dawley rats (100 g, 5 weeks old (Harlen)) underwent an excision of either the forepaw radial nerve (n=4), the forepaw radial and median nerves (n=4), the forepaw radial, median and ulnar nerves (n=4), the hindpaw sciatic nerve (n=5) or the hindpaw sciatic and saphenous nerves (n=10). All these nerves in the rat, contain sensory and

motor fibers, thus severing them removed both efferent and afferent components. Prior to, and at the end of the surgery, buprenorphine (0.01 mg/kg, AmeriSource Bergin) was administered subcutaneously to the rats to prevent stimulation of pain pathways. All surgical procedures were performed under 2% isoflurane anesthesia administrated via a nose cone. Rectal temperature was monitored and maintained at 37°C throughout the surgeries.

The upper and the lower forepaw areas (in case of forepaw deafferentation) or the lateral hip area (in case of hindpaw deafferentation) were shaved and an incision was made in the skin above the target nerve under a dissecting microscope. For the hindpaw deafferentation, the sciatic nerve was cut at the upper-thigh level beneath the medial gluteal muscle and the saphenous nerve cut was performed at the patella level. For the forepaw defferentation, the median nerve was cut underneath the triceps muscles and the radial and ulnar nerves beneath the biceps and pectoral muscles area. A 3.0 mm gap between the distal and the proximal part of the nerve was obtained to insure that no future regeneration of the nerve would take place. All lesions were performed on the right forepaw or hindpaw.

In control rats, the nerves were exposed as described, but were not denervated (sham-nerves operated, n=6). After surgery, the surgical site was closed and the rats were allowed to recover from anesthesia and were monitored for two hours prior to being taken back to the animal facility. During the week following the surgery 1.5ml/100 g of the opioid receptor agonist, Ultram (Tramadol, AmeriSource Bergin), which is used to treat phantom limb pain in humans and animals, was given orally twice a day. An additional dose of Ultram was added into protein-rich jello that was given over night. The rats' weight, food consumption, posture, behavior and overall appearance were monitored daily throughout the study. During the first week following deafferentation, the rats remained active and did not experience any significant weight loss or self-mutilation. However, at the second and the third week following deafferentation, when the Ultram treatment was discontinued, 6 rats that underwent both the sciatic and the saphenous nerves deafferentated, showed self-mutilation on the denervated hindpaw digits. In these rats, Ultram was given again twice a day for 2-3 days. Two of these rats that continued to self-mutilate during the Ultram treatment were euthanized.

Somatosensory cortical lesions—Somatosensory cortical lesions were performed on two separate groups of rats. A week following the sciatic and the saphenous nerves deafferentation (n=5) or the sham procedures (n=5) on the right hindpaw, the right somatosensory cortex hindpaw representation region was stereotaxically lesioned (sciatic and saphenous deafferentation and cortical lesion, and sham-operated and cortical lesion groups, respectively). Prior and at the end of the surgery, 0.01 mg/kg buprenorphine was administrated subcutaneously to the rats.

Two percent isoflurane anesthesia was administered through a nose-cone and the rat's head was secured in a stereotaxic frame. A 1-inch long incision along the midline was made, and the skull was exposed and scraped free of tissue. Using a pneumatic drill, a 1 mm burr hole was made above the somatosensory cortex of the hindpaw representation. A microelectrode (50 μm in diameter) was lowered into the somatosensory region (dorsal- ventral 1.5 mm from dura, medial-lateral 2 mm and anterior-posterior to bregma −1.2 mm). 1 mA current was given continuously for a minute, while the electrode was being moved 0.5 mm in each direction in order to achieve an irreversible localized destruction of the whole hindpaw representation. After the microstimulation procedure, the microelectrode was slowly retracted from the brain, and the burr hole was sealed with bone wax and the tissue above the skull was glued back using tissue glue.

In addition, another control group for the stereotaxic surgery was obtained: a week following the sciatic and saphenous nerves deafferentation, the skin incision along the midline was

performed, but the skull was not drilled and the microelectrode was not lowered into the brain (sciatic and saphenous deafferentation and sham-lesion operated group, n=4).

A week after this surgery, immediately after completing the MRI and euthanizing the animals using a lethal dose of potassium chloride, the brains were removed and placed in parformaldehyde (Sigma) for histology. Staining for cell bodies (Nissl stain) and cell morphology (Hematoxylin and Eosin) were performed on 8 μm paraffin embedded coronal sections (Histoserve) for verifying the localization of the cortical lesions.

Figure 1 shows a diagram demonstrating all the experimental protocols and the timing of the different procedures.

Functional MRI

Rats were initially anesthetized and maintained at 2% isoflurane during the following surgical procedures for MRI. Each rat was orally intubated and placed on a mechanical ventilator throughout the surgery and the experiment. Plastic catheters were inserted into the right femoral artery and vein to allow monitoring of arterial blood gases and administration of drugs. Two needle electrodes were inserted just under the skin of each hindpaw and forepaw, one between digits 1 and 2, and the other between digits 3 and 4. Due to the large distance between the stimulating electrodes to the center of the coils, the stimulation current did not affect the fMRI signal. After surgery, the rat was given an i.v. bolus of 80 mg/kg α-chloralose (Sigma) and isoflurane was discontinued. Anesthesia was maintained with a constant α-chloralose infusion (27 mg/kg/hr) and an i.v. injection of pancuronium bromide (4 mg/kg, AmeriSource Bergin) was given once per hour to prevent motion (Keilholz, 2004; Masamoto, 2006; Silva and Koretsky, 2002).

The rat was placed on a heated water pad to maintain rectal temperature at 37°C while in the MRI. Each animal was secured in a head holder with ear bars and a bite bar to prevent head motion and was strapped to a plastic cradle. End-tidal CO_2, rectal temperature, tidal pressure of ventilation, heart rate, and arterial blood pressure were continuously monitored during the experiment. Arterial blood gas levels were checked periodically and corrections were made by adjusting respiratory volume or administering sodium bicarbonate to maintain normal levels.

All images were acquired on an 11.7 T / 31 cm horizontal bore magnet (Magnex), interfaced to an AVANCE console (Bruker) and equipped with a 9-cm gradient set, capable of providing 64 G/cm with a rise time of 100 μsec (Resonance Research). A linear birdcage coil (inner diameter of 69 mm) was used to transmit and a 20 mm diameter surface coil that was attached to a head holder was used to receive the MR signal. Scout images were acquired in three planes with a fast spin echo sequence to determine appropriate positioning for the functional study. A single-shot, spin-echo, echo-planar imaging (EPI) sequence was run with the following parameters: effective echo time (TE)=30 ms; repetition time (TR)=1.5 sec; bandwidth=200 kHz; a field of view=2.56×2.56 or 1.92×1.92 cm; 64×64 matrix size leading to a nominal in plane resolution of 400 microns or 300 microns. Partial brain coverage was obtained with five, 1 or 2-mm thick slices spaced 0.2 mm apart.

A stimulator (World Precision Instruments) supplied 2.5 mA, 300 μsec pulses repeated at 3 Hz to either the right or the left forepaws or hindpaws upon demand. The paradigm consisted of 10 dummy MRI scans to reach steady state, followed by 40 scans during rest and 10 scans during stimulation, which was repeated four times. The rat was allowed to rest for few minutes between stimulation sets, and three to five sets of data was recorded from each rat for each of the forepaws and hindpaws.

Anatomical MRI

In order to image the precise localization of the somatosensory cortical lesion, T_2 – weighted anatomical images were obtained for each of the lesioned rats. Identical anatomical geometry to the fMRI was used with the following parameters: A RARE sequence with four echoes; slice thickness = 1mm; TE=26 ms; TR=2 sec; bandwidth=200 kHz; a field of view of 2.56×2.56 cm with a 256×256 matrix leading to a nominal in-plane resolution of 100 microns.

Data Analysis

Single animal analysis—Analysis of the fMRI time series for individual animals was performed using STIMULATE (University of Minnesota). A correlation coefficient was calculated from cross-correlation of the unfiltered time series with a boxcar waveform representing the stimulation period. The activation threshold was set at 0.25, and only groups that include at least four activated pixels were considered significant. The number of pixels above this threshold and their averaged amplitude within the appropriate somatosensory representation (forepaw or hindpaw) as was defined by a rat's brain atlas (Paxinos and Watson, 1986) was calculated for each data set. The BOLD percent change with standard deviation (SD) was obtained by calculating the average amplitude during the 4 stimulation epochs subtracted by the average amplitude during rest and divided by the average amplitude during rest. A two-tailed unpaired student T-Test was performed between groups.

Group analysis—Group analysis was performed by custom-written software running in Matlab (MathWorks Inc) and a public domain tool for image registration (http://bishopw.loni.ucla.edu/AIR5/index).

Spatial normalization—To facilitate within and between group comparisons and analysis, the brain images of all animals were normalized to the same spatial dimension. By co-registering all the EPI images to a brain template, the variations in brain sizes and EPI distortions were reduced. The brain EPI image of one normal rat was chosen as the template. Initially, a slice corresponding to the template images was chosen. To avoid the interference from the cortical lesions and skin, brain masks were created manually. The co-registration was performed in two steps using automated image registration (IR, version 5.2.5) to minimize the standard deviation of ratios between two images (Woods, 1998). In order to reduce the gross differences in the brain positions, each image was co-registered to the template by a 2D rigid-body transformation, including two translations and one rotation. The differences in the brain size and distortion were considered in the second step by a two dimensional affine transformation, which further incorporated scaling and shearing. Then the transformation was applied to all images, including different runs, from the same animal using windowed sinc interpolation.

To improve the signal-to-noise ratio and to reduce the residual difference after spatial normalization, images were spatially smoothed by Gaussian filter with full-width-at-half-maximum (FWHM) of 3 pixels. The functional data was analyzed by cross-correlation with respect to the boxcar paradigm with a hemodynamic delay up to 4.5 s (3 scans). Due to the filtering procedure, the threshold was set at correlation coefficient > 0.3 and cluster size > 4 pixels. The within subject reproducibility was checked by the same method for group analysis (see below).

To combine results from individual animals in the same group, the representative data from each animal was re-analyzed by Student *t*-test:

$$t = \frac{\bar{x}_A - \bar{x}_R}{\sqrt{\hat{\sigma}^2\left(1 / N_A + 1 / N_R\right)}}$$

$$\hat{\sigma}^2 = \frac{\left(N_A - 1\right)\sigma_A^2 + \left(N_R - 1\right)\sigma_R^2}{\left(N_A + N_R - 2\right)}$$

[1]

Where $\bar{x}_i$, $\hat{\sigma}_i^2$, and N_i are the mean intensity, variance, and number of time points, respectively, during activated (A) or resting (R) periods. A hemodynamic delay of 1 scan was used and the same spatial smoothing as in the single animal analysis was used. Then group t-score maps were created using a fixed-effects analysis:

$$t = \frac{\bar{\hat{b}}}{\hat{\sigma}_{be} / \sqrt{N}}$$

$$\bar{\hat{b}} = \frac{1}{N} \sum_{i=1}^{N} \hat{b}_i$$

[2]

$$\hat{\sigma}_{be}^2 = \frac{1}{N} \sum_{i=1}^{N} \sigma_{bei}^2$$

Where $\hat{b}_i$ is the mean signal change, i.e., the numerator in Eq. [1], and σ_{bei}^2 is the common variance, i.e., the square of the denominator in Eq. [1], of the ith animal and N is the number of animals in that group. The group t-maps were threshold by $p < 10^{-5}$ (corrected for multiple comparisons by Bonferroni correction).

Results

Forepaw Nerve Deafferentation

In order to study the effect of peripheral nerve deafferentation on cortical reorganization, either a partial denervation of the forepaw (radial nerve or the radial and the median nerves deafferentation) or a complete denervation of the right forepaw (radial, median and ulnar nerves deafferentation) was carried out. All nerves were denervated permanently eliminating any possibility for future regeneration. Previously we demonstrated that following sciatic nerve crush, there is a correlation between the nerve regeneration time course to the return of the fMRI response as a result of the regenerating hindpaw stimulation (Pelled, 2006). Thus, the absence of nerve regeneration following the denervation was directly assessed by the lack of any fMRI response in the deprived cortex when the denervated paw was stimulated.

Figure 2 shows activation maps of individual rats from the three forepaw denervation groups overlaid on EPI MRI images with the corresponding BOLD time courses obtained two weeks following the denervation procedure on the forepaw. Sensory stimulation of the left, intact, forepaw resulted in contralateral SI activation in all of the three groups experiencing different degrees of forepaw denervation (Fig 2 A-C). Stimulation of the intact forepaw in these rats that underwent complete denervation of the right forepaw resulted not only in contralateral SI fMRI activation, but also resulted in ipsilateral SI fMRI activation in the forepaw representation of the denervated paw (Fig 2C). Time courses show fMRI activation in contralateral S1 but not ipsilateral cortex when either the radial or radial and median nerves were cut (Fig 2D and 2E). However, when all three nerves that innervate the forepaw (radial, median and ulnar) were cut there was clear fMRI activation in the time courses in both contralateral and ipsilateral S1 (Fig 2F).

Sensory stimulation of the partial denervated forepaw, as in the radial- denervated and the radial and median- denervated rat groups, resulted in only contralateral SI fMRI activation (data not shown). Sensory stimulation of the forepaw that underwent complete denervation, i.e. radial, median and ulnar- lesion, showed no fMRI activation of the contralateral SI in any of the rats (data not shown).

Figure 3 shows the group averaged t-test maps (n=4 in each group) overlaid on a registered EPI MRI image. Severing only the radial (Fig 3A) or the radial and median nerves (Fig 3B) led only to the appropriate contralateral SI fMRI activation when the healthy paw was stimulated. The percent BOLD signal change was 4.0 ± 0.5 for the radial nerve denervation and 3.25 ± 0.4 for the radial and medial denervation. Only when a complete forepaw denervation was executed did sensory stimulation of the intact forepaw result in both contra- and ipsi- lateral SI fMRI activation (Fig. 3C, $4.0 \pm 1.5\%$ and $2.0 \pm 0.5\%$ BOLD signal change, respectively). Additionally, fMRI activation of part of the secondary somatosensory cortex (SII) was detected on the contralateral hemisphere to the healthy paw (arrow in Fig 3C). Individual activation maps from all animals in each group were checked before calculating the group average to make certain that a similar activation pattern existed between subjects. The significant group activations in these results indicate that they are indeed consistent across the animals and not biased by any individual outlier. However, when calculating the percent signal change, only the averaged signal difference between the stimulation and resting conditions were used. In the group analysis, not only the difference between the two conditions, but also the variance of these conditions was used to calculate the t-value. Therefore, although the average percent signal change was lower in rats that underwent the radial and median nerve deafferentation as compared with rats that underwent only radial deafferentation, the group average map shows higher significance in the latter because the intra-subject variance was larger.

Hindpaw Nerve Deafferentation

To test whether the inter-hemispheric plasticity detected in the forepaw also occurs if similar denervation is performed on a hindpaw, the affect of cutting the sciatic and both the sciatic and saphenous nerves was studied The sciatic nerve was denervated permanently eliminating any possibility for future regeneration. All rats remained active without experiencing any weight loss or self-mutilation. Although in the days following the surgery the rats were dragging the deafferentated hindpaw, two weeks after the deafferentation, the rats had improved their posture, however, flexion and extension of the hindpaw associated with the deafferentated nerve, was not observed in any of the rats, indicating that no sciatic nerve regeneration took place. As compared with the rats that only the sciatic nerve had been deafferentated, the sciatic and the saphenous deafferentated rats were dragging their right (denervated) hindpaw through out the time course of the study and did not show any improvement in posture in the weeks following the surgical procedures while remaining active and increasing their weight. Flexion and extension of the hindpaw associated with the deafferentated nerves, was not observed in any of the rats, indicating that no sciatic nor saphenous nerve regeneration took place. In addition, no fMRI response was observed when the denervated hindpaw was stimulated (data not shown).

Two to three weeks following the sciatic nerve or sciatic and saphenous nerve deafferentation fMRI measurements were obtained. Figure 4 shows the group averaged t-test maps overlaid on a registered EPI MRI image. Sham operated controls showed fMRI activation of the hindpaw SI on the contralateral side to the healthy paw (Fig 4A, $2.2 \pm 0.8\%$ BOLD signal change). The hindpaw area is smaller and shifted more to the mid-line as compared to the forepaw representation. Severing the sciatic nerve and stimulating the healthy paw also led to only contralateral fMRI activation (Fig 4B, $3.0 \pm 0.7\%$ BOLD signal change). When both the sciatic and saphenous nerves were cut there was activation in both the contralateral and

ipsilateral cortex (Fig 4C, 2.3±0.3% BOLD signal change in both hemispheres), consistent with results that were found for the forepaw.

Figure 5 shows t-test value intra-variability maps of an individual sham-operated rat (Fig 5A) and sciatic and saphenous deafferentated rat (Fig 5B). Three to four stimulation sets of fMRI data were acquired from each individual rat enabling the variability of the cortical response within an individual rat to be assessed. The map demonstrates that following the intact hindpaw stimulation, fMRI activation of the ipsilateral SI in addition to the contralateral SI was observed in each single fMRI session in the sciatic and saphenous nerves denervated rat. The variation of the BOLD signal within an individual animal was smaller compared to the variability between subjects. Therefore, the P values of the consistency maps are smaller compared to the group average (Fig 4) indicating reproducibility of the activated area in an individual animal.

Quantification of Results from Forepaw and Hindpaw fMRI Studies

Table 1 shows the group average of the number of pixels in the intact and the deprived SI as was calculated from the cross correlation maps for each of the six groups of rats participating in this study (cc>0.25). In all these cases, the number of pixels was calculated in response to stimulation of the left (healthy) limb. Partial denervation of the rat's forepaw did not result in any significant change in SI fMRI activation area. However, complete denervation of the rat's forepaw or hindpaw resulted in bilateral cortical fMRI activation when the healthy, intact forepaw was stimulated. In both cases, the size of the ipsilateral activation that occurs when the healthy paw was stimulated led to fMRI activation of approximately 25% (in case of forepaw denervation) or 50% (in case of hindpaw denervation) of the representation on the contralateral side.

Somatosensory cortical lesions

Irreversible stereotaxic ablation of the right SI hindpaw representation was performed in sham-operated and sciatic and saphenous denervated rats for investigating whether the bilateral somatosensory activity that was observed in the sciatic and saphenous deafferentated rats required the healthy SI cortex. The hindpaw was used rather than the forepaw because it has a smaller representation making it easier to ablate. Stereotaxic cortical lesions were executed on the right SI cortical area, contralateral to the healthy hindpaw. The anatomical location of the lesions was confirmed using both high resolution anatomical MRI mapping and histology as demonstrated in Figure 6. In order to visualize if following the cortical lesion procedure any additional anatomical damage had occurred, such as brain edema, T_2-weighted contrast was obtained. A small focal lesion in the hindpaw representation was clearly evident from the MRI and the histology in all rats. To ensure that the lesion was localized to the hindpaw region, fMRI was acquired while stimulating either the healthy hindpaw that innervated the lesioned cortex or the forepaw on the same side. There was no fMRI detected in the lesioned cortex (data not shown). Figure 7 shows that in rats that had lesions in the hindpaw representation and were either control (Fig 7A) or had the sciatic and saphenous nerves severed (Fig 7B) there was robust fMRI response in the forepaw SI when the forepaw was stimulated. Fig 7C shows a typical fMRI time course from the forepaw representation. This result indicates that the lesion in the hindpaw representation of SI did not damage the neighboring forepaw SI. In 95% of all rats that underwent the stereotaxic cortical lesions, the cortical lesion was found to be located precisely in the SI cortical hindpaw representation, and did not affect the forepaw cortical representation. Only rats with a focal lesion in the hindpaw representation that did not affect the forepaw region were used.

Figure 8 shows that ablation of the healthy hindpaw cortex eliminates the ipsilateral activity detected after deafferentation of the sciatic and saphenous nerves. Fig 8A shows data from rats that were sham operated for deafferentation of the sciatic and saphenous nerve but had a cortical

lesion in the healthy hindpaw SI. No fMRI activation in the contralateral SI was detected when the healthy paw was stimulated indicating the lesion was affective in ablating SI cortex. Stimulation of the forepaws or the sham operated hindpaw led to fMRI activation in the appropriate SI representation (data not shown). The top row shows results from an individual rat and the bottom row shows group averaged results from five rats.

Fig 8B shows that in rats that had the sciatic and saphenous nerves cut and a cortical lesion in the healthy hindpaw SI, there was no fMRI activation in either the lesioned contralateral SI or the ipsilateral SI when the intact hindpaw was stimulated. There was fMRI activation in both forepaw SI representations when the healthy forepaws were stimulated (data not shown). Similarly, the top row shows results from an individual rat and the bottom row shows group averaged results from 5 rats.

Fig 8C shows the bilateral fMRI activation obtained when the healthy paw was stimulated two weeks following cutting the sciatic and saphenous nerves in rats that were sham operated for the cortical lesion. Stimulation of the healthy forepaws resulted in normal contralateral SI fMRI activation (data not shown). The top row shows results from an individual rat and the bottom row shows group averaged results from the five rats. These results indicate that the SI cortical representation of the healthy paw is essential for the inter-hemispheric cortical reorganization that leads to ipsilateral fMRI activation when the healthy paw is stimulated after complete denervation of the hindpaw.

Discussion

Recently, there has been growing evidence from human fMRI studies that there can be large scale cortical-cortical plasticity associated with damage. Indeed, in Braille readers blind from birth, somatosensory stimulation of the fingers during Braille reading leads to activation of visual cortex (Sadato, 1996). More recently, damage to cortex due to stroke has been shown to cause interhemispheric plasticity causing bilateral fMRI activation when the healthy cortex is activated by stimulation of the appropriate body part (Kim, 2003). In addition, acute peripheral nerve deafferentation was shown to elicit bilateral cortical responses in human motor cortex (Werhahn, 2003). Furthermore, it has been shown that lesions caused by stroke specific to thalamus led to bilateral fMRI activation when electrical stimulation was applied to digits innervating the unaffected thalamus (Taskin, 2005). Inspired by these human imaging results, but wanting to work in a model system more amenable to understanding the mechanism of inter-hemispheric plasticity, we tested whether peripheral nerve deafferentation leads to inter-hemispheric cortical reorganization in the rat.

In the present study the consequences of peripheral nerve deafferentation on cortical reorganization in rodent SI was explored. Specifically, fMRI was used to address whether peripheral nerve deafferentation modulates inter-hemispheric responses reflecting a reorganization of deprived cortical areas. The long-term consequences of partial and complete limb denervation on SI cortical responses were studied. Sensory stimulation of the partial denervated forepaw showed only normal, contralateral SI fMRI activation when the good forepaw was stimulated. There was a trend to a smaller region activated but this did not reach statistical significance. Interestingly, bilateral cortical fMRI activation in both the contralateral as well as in the ipsilateral SI was detected when the healthy forepaw was stimulated only in rats that underwent complete forepaw denervation. When bilateral fMRI activation occurred, responses were reproducible, although the averaged BOLD amplitude of the deprived cortex was reduced significantly compare to the amplitude of the contralateral cortex to the stimulated healthy forepaw. In addition, only about 25% of the number of pixels showed fMRI activation indicating that about a quarter of the representation was affected by inter-hemispheric cortical reorganization.

Similarly, in the hindpaw deafferentation rat model, it took complete denervation of the hindpaw by cutting the sciatic and saphenous nerves to get significant fMRI evidence of bilateral cortical reorganization. When all input from one hindpaw was eliminated, then stimulation of the healthy hindpaw led to bilateral fMRI activation in the normal, contralateral SI as well as the ipsilateral SI region. The amplitude of fMRI response was larger in the deprived hindpaw SI compared to the deprived forepaw SI. In addition, the region affected was larger with respect to the normal SI representation in the deprived hindpaw SI as compared to the deprived forepaw SI. Therefore, in order for the deprived cortex to have detectable fMRI activation in the ipsilateral cortex to the healthy limb, there must be a complete lack of sensory input from the contralateral limb to the brain.

There is evidence of interhemispheric communication in a number of animal models of temporary and chronic nerve deafferentation. The short term affects of temporary and partial peripheral deafferentation on cortical plasticity have been studied in the flying fox (Calford and Tweedale, 1990) macaque monkey (Calford and Tweedale, 1990) and rat (Shin, 1997). In these studies, a digit was temporarily paralyzed with local anesthetic after that digits receptive field was mapped. After paralyzing the digit, the contralateral and ipsilateral receptive fields to a neighboring digit was mapped minutes following drug application. The lack of sensory input from the paralyzed digit was immediately reflected upon the expansion of the neighboring digit's receptive field into the paralyzed digits receptive field in the appropriate, contralateral cortex as is typical for intra-cortical plasticity. Interestingly, there were changes in the homologous, neighboring digits receptive field on the opposite limb. The receptive field also increased in this digit's appropriate contralateral cortical representation even though the neighboring digit was normal. Thus, the paralyzed digit caused changes in receptive fields in both its contralateral and ipsilateral cortex. This occurred even though the neurons that displayed enlarged receptive fields were not responsive to ipsilateral stimulation.

Other studies indicate that temporary and acute inactivation of SI cortex resulted in receptive field enlargement in the contralateral (healthy) SI representation when an appropriate body part was stimulated (Clarey, 1996; Reinecke, 2003; Rema and Ebner, 2003). There is evidence that a percentage of neurons in the rat SI representation of the limbs have bilateral receptive fields (Armstrong-James and George, 1988) whereas the percent of the neurons exhibiting bilateral receptive fields changed according to the anesthesia depth. Taken together, this body of work, including the new results reported here, clearly demonstrates strong interhemispheric influences and point out that when the balance between excitatory and inhibitory input is modulated in SI the consequences can be quickly reflected in the homologous region in the contralateral SI.

The mechanism and the time course of the interhemispheric cortical reorganization with respect to recovery of the affected limb following stroke remains unclear. Human studies demonstrated that inappropriate fMRI response in the unaffected hemisphere when the affected hand is being stimulated can persists up to few months although recovery of the affected hand was observed (Feydy, 2002; Kim, 2003). Furthermore, in analogy to human studies, damage caused by stroke to rat SI cortex led to bilateral fMRI activation when the paw that normally activates the unaffected cortex was stimulated two weeks following stroke (Abo, 2001; Kim, 2005). However, Dijkhuizen and colleagues (Dijkhuizen, 2001) demonstrated that although strong bilateral fMRI activation was observed at the days following the stroke, this phenomena was reduced over the course of 3 weeks. In the present study the effect of peripheral injury was studied 2-3 weeks following surgical procedures. Preliminary data indicates that the ipsilateral activation developed as early as 7 days. The detailed development of the interhemispheric reorganization warrants further study.

In the past decade α—chloralose has been widely used in rodents for fMRI studies, because the neurovascular coupling which is required for the hemodynamic signal for fMRI is preserved (Hyder, 2002; Masamoto, 2006; Silva and Koretsky, 2002; Ueki, 1992). It is possible that anesthesia alters responses that may occur in the unanesthetized brain and so the results indicating bilateral cortical fMRI activation detected under α—chloralose may be affected by this choice of anesthetic. Unfortunately, α—chloralose (or urethane) has been the only anesthetics to give reproducible fMRI results across a number of laboratories. There are isolated reports of rodent fMRI under other anesthetics such as domitor (Weber, 2006) or isofluorane (Masamoto, 2006) as well as in awake rodents (Lahti, 1998; Pelled, 2002), but none of these other protocols has found widespread use. In addition to its ill defined effects on neural activity, another major disadvantage of using α—chloralose is that it is unsuitable for longitudinal studies. A final problem with rodent fMRI is that robust responses are only detected in SI. FMRI responses in brain regions other then the primary somatosensory cortex such as SII or thalamus are only observed a small percent of the time (Keilholz, 2004; Masamoto, 2006; Ogawa, 2000; Silva and Koretsky, 2002). It is not clear why this is the case it may be that small variations in the anesthetic depth might account for the appearance of the fMRI response in those regions or because the neural representation in these regions is below the resolution or sensitivity of present rodent fMRI.

An important issue for these studies is whether to interpret the fMRI activation as net excitation or inhibition in the ipsilateral cortex to the healthy paw. Although there is a complex relationship between the hemodynamic response detected by BOLD and neuronal activity, the bulk of the evidence is that robust fMRI responses only occur when there is cortical excitation (Brinker, 1999; Duong, 2001; Logothetis, 2001). It has been argued that inhibitory interneurons contribute to local energy consumption, and consequently should cause vasodilation and changes to the BOLD signal (Waldvogel, 2000). An increase in blood flow in cerebellum has been detected during inhibition (Lauritzen, 2001) and a BOLD response in monkey cortex has been attributed to inhibition based on electrophysiological evidence (Lipton, 2006). In addition, it was recently demonstrated that evoked firing of a specific subset of γ-aminobutyric acid interneurons can induce dilatation or constriction of local microvessels (Cauli, 2004; Hamel, 2006) A study in humans specifically attempted to see if inhibitory activity alone could elicit a BOLD response in human somatosensory and motor cortex but did not detect significant BOLD activation although there was clear evidence for neuronal inhibition (Waldvogel, 2000). Under what circumstances fMRI activation occurs when there is net inhibition in an area remains an open issue. In many fMRI papers inhibitory inputs are inferred from decreases in fMRI activation (Ogawa, 2000) or if the signal decrease correlate to the stimulation paradigm (Shmuel, 2006).

In the normal rat the input across hemispheres from homologous S1 areas leads to inhibition (Kandel and Buzsaki, 1997). There has been no report of significant fMRI activation in cortex ipsilateral to an activated limb in the normal rat despite the large amount of work using fMRI in rodents (Keilholz, 2004; Kim, 2000; Kim and Ugurbil, 1997; Silva and Koretsky, 2002).

Nevertheless, all the above works were conducted on healthy human and animal brains. It is believed that the cortical somatosensory maps boundaries in the normal state are maintained by a balance between excitatory input and local inhibitory circuits (Higley and Contreras, 2006). It has been demonstrated previously that this neuronal balance could be severely disturbed in pathological states, leading to short- and long-term reorganization changes of SI (Maffei, 2006; Schierloh, 2003, 2004). Therefore, it remains a possibility that the complete denervation of the forepaw and hindpaw led to increase in inhibitory activity that elicited an fMRI response. Future studies will verify whether the fMRI response detected is due to net excitation or inhibition using electrophysiological and pharmacological manipulations of the complicated cortical excitatory and inhibitory network.

In the present studies, irreversible ablation of the SI cortex contralateral to the healthy paw was used to assess the importance of this area in mediating fMRI activation in the ipsilateral cortex. Ablation of the healthy SI completely abolished fMRI activation of the deprived, ipsilateral SI area when the intact hindpaw was stimulated. If activation of the deprived SI was still present after cortical ablation it would have suggested that reorganization in sub-cortical regions was the foundation of the ipsilateral SI activation. Therefore, it is most likely that the primary contribution for the fMRI activation in the ipsilateral SI arises from inputs originating in the contralateral SI, probably via the corpus callosum, which is the principal anterior intercortical connective pathway (Aboitiz and Montiel, 2003; Innocenti, 1994; Wise and Jones, 1978).

Sub-cortical regions that are engaged with the spinothalamic and medial laminiscus tracts such as the ventroposterior-lateral thalamic nuclei (VPL), have been shown to contribute to intrahemispheric cortical reorganization in adjacent areas following limb deafferentation (Jones, 2000; Krupa, 1999; Stojic, 1998; Wise and Jones, 1978). However, previous studies using retrograde and anterograde labeling methods have demonstrated that the topographical synaptic organization in these nuclei are very specific, and no contralateral VPL-SI projections have been found (Dykes, 1988; Wise and Jones, 1978). Although modifications of synaptic strength and synaptic architecture might occur following deafferentation in sub-cortical structures, they are probably not the foundation of bilateral SI activation following limb deafferentation.

In conclusion, total denervation of a forepaw or a hindlimb leads to interhemispheric reorganization in the rodent primary somatosensory cortex. Stimulation of the normal limb leads to fMRI activation in the normal, contralateral somatosensory cortex. In addition there is fMRI activation of the ipsilateral somatosensory cortex which occupied approximately 25% of the normal representation. The bilateral fMRI activation was only detected when all of the nerves innervating the forepaw or hindpaw were cut indicating that it requires a complete absence of excitatory input to the ipsilateral (to the healthy paw) cortex. Furthermore, ablation of the cortex, contralateral to the healthy paw abolishes the ipsilateral activation indicating that the healthy cortex is essential for the interhemispheric cortical reorganization detected.

References

Abo M, Chen Z, Lai LJ, Reese T, Bjelke B. Functional recovery after brain lesion--contralateral neuromodulation: an fMRI study. Neuroreport 2001;12:1543–1547. [PubMed: 11388445]

Aboitiz F, Montiel J. One hundred million years of interhemispheric communication: the history of the corpus callosum. Braz J Med Biol Res 2003;36:409–420. [PubMed: 12700818]

Armstrong-James M, George MJ. Bilateral receptive fields of cells in rat Sm1 cortex. Exp Brain Res 1988;70:155–165. [PubMed: 3402562]

Borsook D, Becerra L, Fishman S, Edwards A, Jennings CL, Stojanovic M, Papinicolas L, Ramachandran VS, Gonzalez RG, Breiter H. Acute plasticity in the human somatosensory cortex following amputation. Neuroreport 1998;9:1013–1017. [PubMed: 9601659]

Brinker G, Bock C, Busch E, Krep H, Hossmann KA, Hoehn-Berlage M. Simultaneous recording of evoked potentials and T2*-weighted MR images during somatosensory stimulation of rat. Magn Reson Med 1999;41:469–473. [PubMed: 10204868]

Calford MB, Tweedale R. Interhemispheric transfer of plasticity in the cerebral cortex. Science 1990;249:805–807. [PubMed: 2389146]

Caramia MD, Iani C, Bernardi G. Cerebral plasticity after stroke as revealed by ipsilateral responses to magnetic stimulation. Neuroreport 1996;7:1756–1760. [PubMed: 8905658]

Cauli B, Tong XK, Rancillac A, Serluca N, Lambolez B, Rossier J, Hamel E. Cortical GABA interneurons in neurovascular coupling: relays for subcortical vasoactive pathways. J Neurosci 2004;24:8940–8949. [PubMed: 15483113]

Chen R, Cohen LG, Hallett M. Nervous system reorganization following injury. Neuroscience 2002;111:761–773. [PubMed: 12031403]

Clarey JC, Tweedale R, Calford MB. Interhemispheric modulation of somatosensory receptive fields: evidence for plasticity in primary somatosensory cortex. Cereb Cortex 1996;6:196–206. [PubMed: 8670650]

Darian-Smith C, Gilbert CD. Axonal sprouting accompanies functional reorganization in adult cat striate cortex. Nature 1994;368:737–740. [PubMed: 8152484]

Dijkhuizen RM, Ren J, Mandeville JB, Wu O, Ozdag FM, Moskowitz MA, Rosen BR, Finklestein SP. Functional magnetic resonance imaging of reorganization in rat brain after stroke. Proc Natl Acad Sci U S A 2001;98:12766–12771. [PubMed: 11606760]

Duong TQ, Kim DS, Ugurbil K, Kim SG. Localized cerebral blood flow response at submillimeter columnar resolution. Proc Natl Acad Sci USA 2001;98:10904. [PubMed: 11526212]

Dykes RW, Landry P, Hicks TP, Diadori P, Metherate R. Specificity of connections in the ventroposterior nuclei of the thalamus. Prog Neurobiol 1988;30:87–103. [PubMed: 3275408]

Feydy A, Carlier R, Roby-Brami A, Bussel B, Cazalis F, Pierot L, Burnod Y, Maier MA. Longitudinal study of motor recovery after stroke: recruitment and focusing of brain activation. Stroke 2002;33:1610–1617. [PubMed: 12053000]

Hamel E. Perivascular nerves and the regulation of cerebrovascular tone. J Appl Physiol 2006;100:1059–1064. [PubMed: 16467392]

Higley MJ, Contreras D. Balanced excitation and inhibition determine spike timing during frequency adaptation. J Neurosci 2006;26:448–457. [PubMed: 16407542]

Hyder F, Rothman DL, Shulman RG. Total neuroenergetics support localized brain activity: implications for the interpretation of fMRI. Proc Natl Acad Sci U S A 2002;99:10771–10776. [PubMed: 12134057]

Innocenti GM. Some new trends in the study of the corpus callosum. Behav Brain Res 1994;64:1–8. [PubMed: 7840876]

Jones EG. Cortical and subcortical contributions to activity-dependent plasticity in primate somatosensory cortex. Annu Rev Neurosci 2000;23:1–37. [PubMed: 10845057]

Kaas JH, Florence SL, Jain N. Subcortical contributions to massive cortical reorganizations. Neuron 1999;22:657–660. [PubMed: 10230786]

Kandel A, Buzsaki G. Cellular-synaptic generation of sleep spindles, spike-and-wave discharges, and evoked thalamocortical responses in the neocortex of the rat. J Neurosci 1997;17:6783–6797. [PubMed: 9254689]

Keilholz SD, Silva AC, Raman M, Merkle H, Koretsky AP. Functional MRI of the rodent somatosensory pathway using multislice echo planar imaging. Magn Reson Med 2004;52:89–99. [PubMed: 15236371]

Kim DS, Duong TQ, Kim SG. High-resolution mapping of iso-orientation columns by fMRI. Nat Neurosci 2000;3:164–169. [PubMed: 10649572]

Kim SG, Ugurbil K. Comparison of blood oxygenation and cerebral blood flow effects in fMRI: estimation of relative oxygen consumption change. Magn Reson Med 1997;38:59–65. [PubMed: 9211380]

Kim YH, Jang SH, Chang Y, Byun WM, Son S, Ahn SH. Bilateral primary sensori-motor cortex activation of post-stroke mirror movements: an fMRI study. Neuroreport 2003;14:1329–1332. [PubMed: 12876467]

Kim YR, Huang IJ, Lee SR, Tejima E, Mandeville JB, van Meer MP, Dai G, Choi YW, Dijkhuizen RM, Lo EH, Rosen BR. Measurements of BOLD/CBV ratio show altered fMRI hemodynamics during stroke recovery in rats. J Cereb Blood Flow Metab 2005;25:820–829. [PubMed: 15758949]

Krupa DJ, Ghazanfar AA, Nicolelis MA. Immediate thalamic sensory plasticity depends on corticothalamic feedback. Proc Natl Acad Sci U S A 1999;96:8200–8205. [PubMed: 10393972]

Lahti KM, Ferris CF, Li F, Sotak CH, King JA. Imaging brain activity in conscious animals using functional MRI. J Neurosci Methods 1998;82:75–83. [PubMed: 10223517]

Lauritzen M. Relationship of spikes, synaptic activity, and local changes of cerebral blood flow. J Cereb Blood Flow Metab 2001;21:1367–1383. [PubMed: 11740198]

Lipton ML, Fu KM, Branch CA, Schroeder CE. Ipsilateral hand input to area 3b revealed by converging hemodynamic and electrophysiological analyses in macaque monkeys. J Neurosci 2006;26:180–185. [PubMed: 16399685]

Logothetis NK, Pauls J, Augath M, Trinath T, Oeltermann A. Neurophysiological investigation of the basis of the fMRI signal. Nature 2001;412(6843):150–157. [PubMed: 11449264]

Luke LM, Allred RP, Jones TA. Unilateral ischemic sensorimotor cortical damage induces contralesional synaptogenesis and enhances skilled reaching with the ipsilateral forelimb in adult male rats. Synapse 2004;54:187–199. [PubMed: 15472929]

Maffei A, Nataraj K, Nelson SB, Turrigiano GG. Potentiation of cortical inhibition by visual deprivation. Nature 2006;443:81–84. [PubMed: 16929304]

Mandeville JB, Marota JJ, Kosofsky BE, Keltner JR, Weissleder R, Rosen BR, Weisskoff RM. Dynamic functional imaging of relative cerebral blood volume during rat forepaw stimulation. Magn Reson Med 1998;39:615–624. [PubMed: 9543424]

Masamoto K, Kim T, Fukuda M, Wang P, Kim SG. Relationship between Neural, Vascular, and BOLD Signals in Isoflurane-Anesthetized Rat Somatosensory Cortex. Cereb Cortex. 2006

Melzer P, Smith CB. Plasticity of cerebral metabolic whisker maps in adult mice after whisker follicle removal--I. Modifications in barrel cortex coincide with reorganization of follicular innervation. Neuroscience 1998;83:27–41. [PubMed: 9466397]

Merzenich MM, Kaas JH, Wall JT, Sur M, Nelson RJ, Felleman DJ. Progression of change following median nerve section in the cortical representation of the hand in areas 3b and 1 in adult owl and squirrel monkeys. Neuroscience 1983;10:639–665. [PubMed: 6646426]

Metzler J, Marks PS. Functional changes in cat somatic sensory-motor cortex during short-term reversible epidural blocks. Brain Res 1979;177:379–383. [PubMed: 497840]

Ogawa S, Lee TM, Stepnoski R, Chen W, Zhu XH, Ugurbil K. An approach to probe some neural systems interaction by functional MRI at neural time scale down to milliseconds. Proc Natl Acad Sci USA 2000;97:11026–11031. [PubMed: 11005873]

Ogawa S, Lee TM, Stepnoski R, Chen W, Zhu XH, Ugurbil K. An approach to probe some neural systems interaction by functional MRI at neural time scale down to milliseconds. Proc Natl Acad Sci USA 2000;97:11026. [PubMed: 11005873]

Paxinos, G.; Watson, C. The rat brain in stereotaxic coordinates. Academic Press; Sydney; New York: 1986.

Pelled G, Bergman H, Goelman G. Bilateral overactivation of the sensorimotor cortex in the unilateral rodent model of Parkinson's disease - a functional magnetic resonance imaging study. Eur J Neurosci 2002;15:389–394. [PubMed: 11849305]

Pelled G, Dodd SJ, Koretsky AP. Catheter confocal fluorescence imaging and functional magnetic resonance imaging of local and systems level recovery in the regenerating rodent sciatic nerve. Neuroimage 2006;30:847–856. [PubMed: 16343952]

Reinecke S, Dinse HR, Reinke H, Witte OW. Induction of bilateral plasticity in sensory cortical maps by small unilateral cortical infarcts in rats. Eur J Neurosci 2003;17:623–627. [PubMed: 12581180]

Rema V, Ebner FF. Lesions of mature barrel field cortex interfere with sensory processing and plasticity in connected areas of the contralateral hemisphere. J Neurosci 2003;23:10378–10387. [PubMed: 14614097]

Sadato N, Pascual-Leone A, Grafman J, Ibanez V, Deiber MP, Dold G, Hallett M. Activation of the primary visual cortex by Braille reading in blind subjects. Nature 1996;380:526–528. [PubMed: 8606771]

Schierloh A, Eder M, Zieglgansberger W, Dodt HU. Sensory deprivation changes the pattern of synaptic connectivity in rat barrel cortex. Neuroreport 2003;14:1787–1791. [PubMed: 14534421]

Schierloh A, Eder M, Zieglgansberger W, Dodt HU. Effects of sensory deprivation on columnar organization of neuronal circuits in the rat barrel cortex. Eur J Neurosci 2004;20:1118–1124. [PubMed: 15305882]

Shin HC, Won CK, Jung SC, Oh S, Park S, Sohn JH. Interhemispheric modulation of sensory transmission in the primary somatosensory cortex of rats. Neurosci Lett 1997;230:137–139. [PubMed: 9259483]

Shir Y, Sheth R, Campbell JN, Raja SN, Seltzer Z. Soy-containing diet suppresses chronic neuropathic sensory disorders in rats. Anesth Analg 2001;92:1029–1034. [PubMed: 11273945]

Shmuel A, Augath M, Oeltermann A, Logothetis NK. Negative functional MRI response correlates with decreases in neuronal activity in monkey visual area V1. Nat Neurosci 2006;9:569–577. [PubMed: 16547508]

Silva AC, Koretsky AP. Laminar specificity of functional MRI onset times during somatosensory stimulation in rat. Proc Natl Acad Sci USA 2002;99:15182–15187. [PubMed: 12407177]

Stojic AS, Lane RD, Killackey HP, Qadri BA, Rhoades RW. Thalamocortical and intracortical projections to the forelimb-stump SI representation of rats that sustained neonatal forelimb removal. J Comp Neurol 1998;401:187–204. [PubMed: 9822148]

Taskin B, Jungehulsing GJ, Ruben J, Brunecker P, Krause T, Blankenburg F, Villringer A. Preserved Responsiveness of Secondary Somatosensory Cortex in Patients with Thalamic Stroke. Cereb Cortex. 2005

Ueki M, Mies G, Hossmann KA. Effect of alpha-chloralose, halothane, pentobarbital and nitrous oxide anesthesia on metabolic coupling in somatosensory cortex of rat. Acta Anaesthesiol Scand 1992;36:318–322. [PubMed: 1595336]

Verley R, Onnen I. Somatotopic organization of the tactile thalamus in normal adult and developing mice and in adult mice dewhiskered since birth. Exp Neurol 1981;72:462–474. [PubMed: 7238702]

Verney C, Farkas-Bargeton E, Verley R. Reorganization of thalamo-cortical connections in mice dewhiskered since birth. Neurosci Lett 1982;32:265–270. [PubMed: 7177490]

Waldvogel D, van Gelderen P, Muellbacher W, Ziemann U, Immisch I, Hallett M. The relative metabolic demand of inhibition and excitation. Nature 2000;406:995–998. [PubMed: 10984053]

Wall JT, Cusick CG. Cutaneous responsiveness in primary somatosensory (S-I) hindpaw cortex before and after partial hindpaw deafferentation in adult rats. J Neurosci 1984;4:1499–1515. [PubMed: 6726345]

Weber R, Ramos-Cabrer P, Wiedermann D, van Camp N, Hoehn M. A fully noninvasive and robust experimental protocol for longitudinal fMRI studies in the rat. Neuroimage 2006;29:1303–1310. [PubMed: 16223588]

Werhahn KJ, Mortensen J, Van Boven RW, Cohen LG. Bihemispheric plasticity after acute hand deafferentation. Suppl Clin Neurophysiol 2003;56:232–241. [PubMed: 14677400]

Wise SP, Jones EG. Developmental studies of thalamocortical and commissural connections in the rat somatic sensory cortex. J Comp Neurol 1978;178:187–208. [PubMed: 627623]

Woods RP, Grafton ST, Watson JD, Sicotte NL, Mazziotta JC. Automated image registration: II. Intersubject validation of linear and nonlinear models. J Comput Assist Tomogr 1998;22:153–165. [PubMed: 9448780]
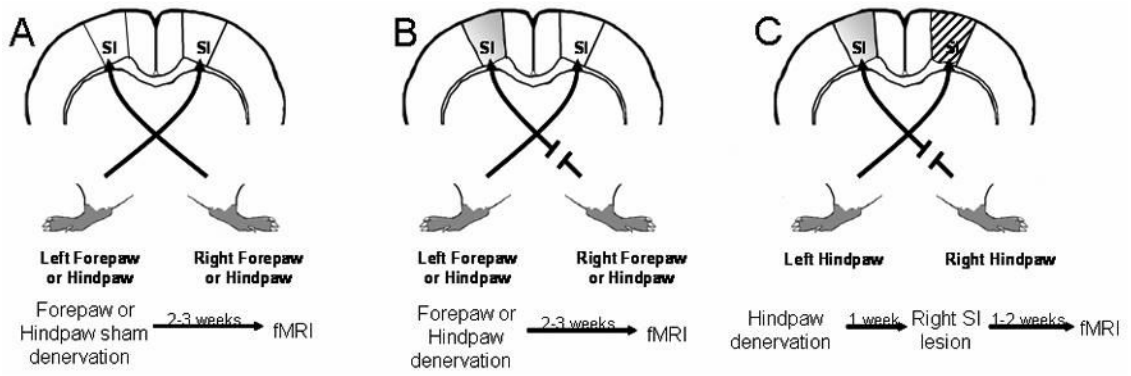
Figure 1.
A diagram of the experimental protocols and the timing of the different procedures. (A) Under normal conditions and in the sham-operated rats the majority of the sensory afferent innervates the contralateral primary somatosensory cortex (SI). Therefore, the right forepaw or hindpaw activates the left or the right SI, respectively, and *vice versa*. (B) Rats underwent a partial or a complete denervation of either the right forepaw or the hindpaw, 2-3 weeks before fMRI measurements. Shaded area represents the deprived SI (contralateral to the denervated paw, ipsilateral to the healthy paw). (C) In addition to a complete right hindpaw nerves denervation, an additional group or rats underwent stereootaxic ablation of the healthy paw's SI cortex (right SI of the hindpaw representation, ipsilateral to the denervated hindpaw) represented by the striped area.
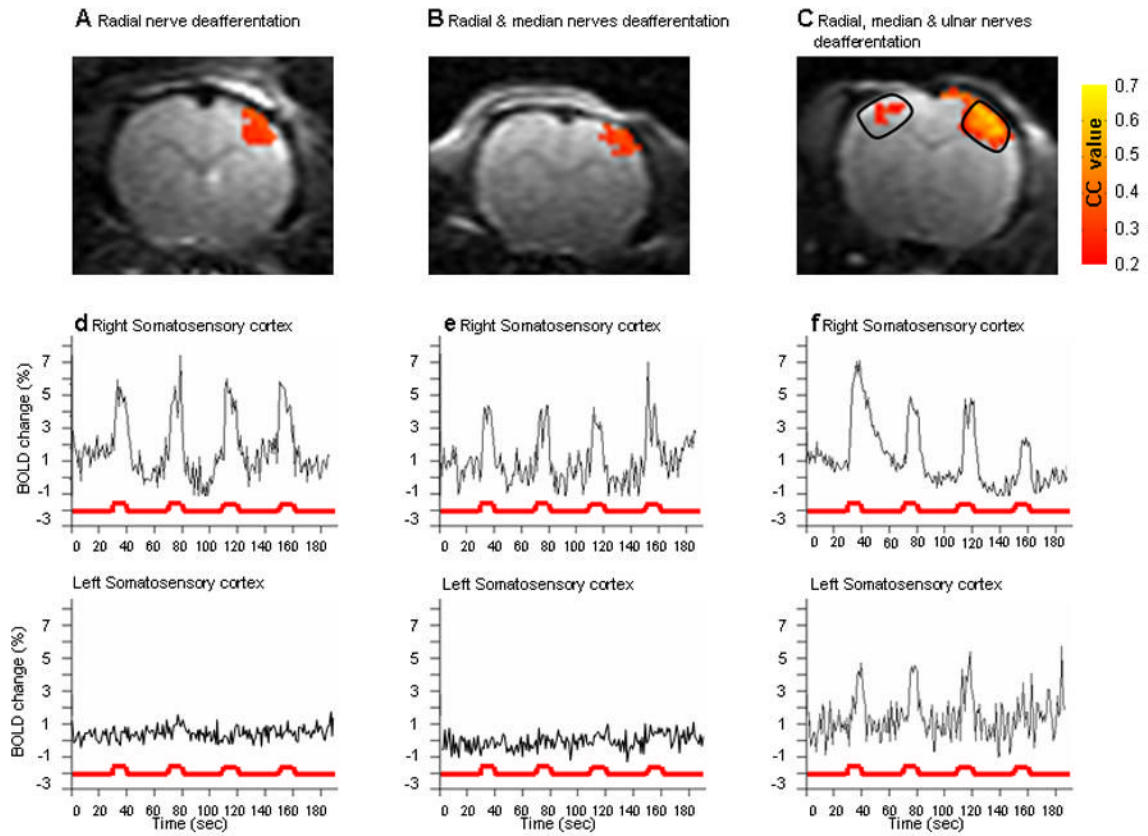
Figure 2.
Representative activation maps and time courses of BOLD responses to intact forepaw stimulation. Representative activation maps calculated from cross correlation of p>0.25 overlaid on the original EPI images from three individual rats from each of the groups (A) Radial nerve deafferentation, (B) Radial and median nerves deafferentation and (C) Radial, median and ulnar nerves deafferentation. The BOLD time course of the contra- and the ipsi-lateral primary somatosensory cortex as a response to the intact forepaw stimulation is illustrated for the each of the radial nerve deafferentated rat (D) the radial and median nerves deafferentated rat (E) and for the radial, median and ulnar nerves deafferentated rat (F). Only in the radial, median and ulnar nerves deafferentated rat, intact forepaw stimulation resulted with both contra- and ipsi-lateral somatosensory activation. BOLD time courses were calculated from a defined region of interest, as was determined by a rat brain anatomy atlas (as illustrated in (C)) in the right and the left somatosensory cortex of the rats presented in the upper row.
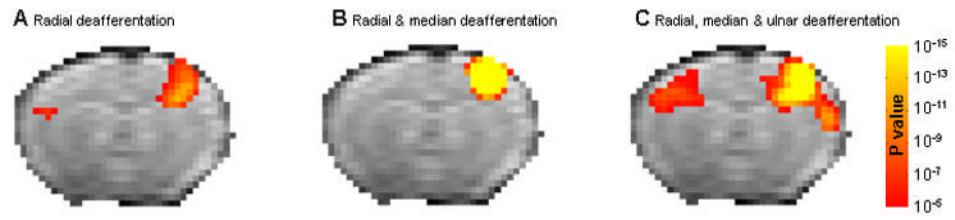
Figure 3.
Group activation t-test maps. Group t-test maps ($p<10^{-5}$, corrected for multiple comparison) overlaid on the EPI template image for the (A) Radial nerve deafferentated rats (n=4), (B) Radial and median nerves deafferentated rats (n=4) and (C) Radial, median and ulnar nerves deafferentated rats (n=4). Arrow points out secondary somatosensory area.
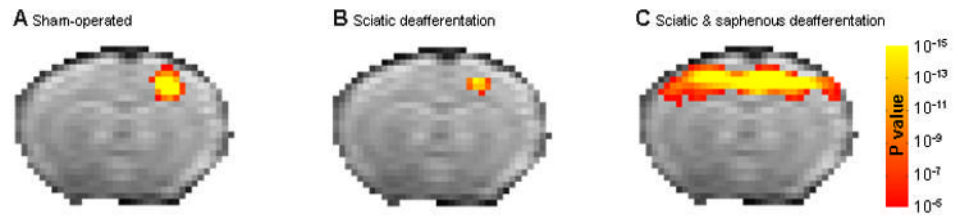
Figure 4.
Group activation t-test maps. Group t-test maps (p<10^{-5}, corrected for multiple comparison) overlaid on the EPI template image for the (A) Sham-operated rats (n=5), (B) Sciatic nerve deafferentated rats (n=5) and (C) Sciatic and saphenous nerves deafferentated rats (n=8).
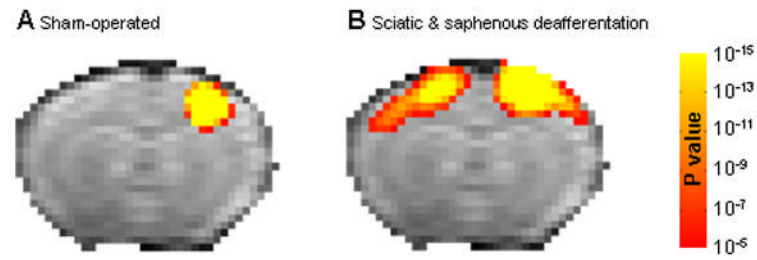
Figure 5.
Intra-variability t-test maps. Intra-variability t-test maps overlaid on an EPI template image of individuals sham-operated (A) and sciatic and saphenous nerve deafferentated (B) rats which integrated 3 single t-test maps created from 3 single sets acquired after sensory stimulation of the intact hindpaw. The maps demonstrate the reproducibility of the bilateral activation following intact hindpaw stimulation phenomena within an individual sciatic and saphenous nerve deafferentated rat.
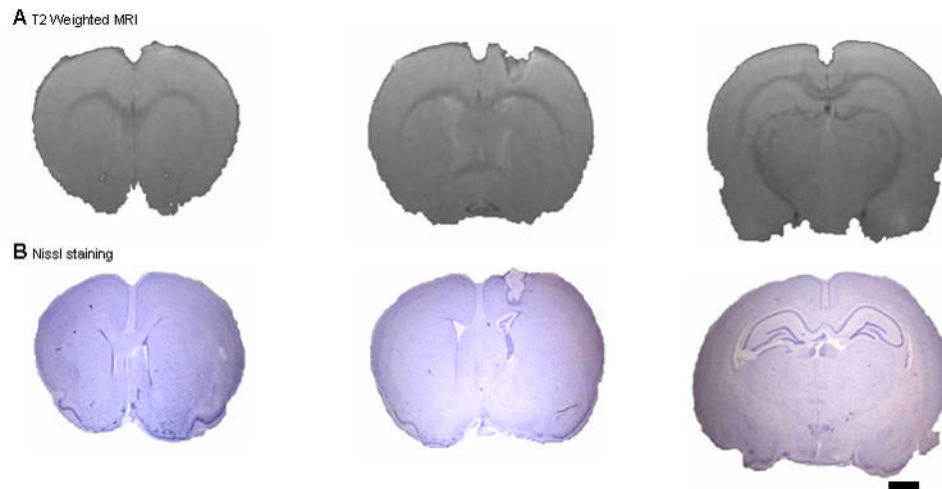
Figure 6.
Anatomical MRI and Nissl stains of the somatosensory hindpaw cortical representation lesions. (A) High-resolution (100 × 100 μm) T2 weighted MRI images and (B) Nissl stains of a representative rat that underwent somatosensory cortical ablation of the hindpaw representation. The lesion can be clearly identified and localized using both methods. Anterior and posterior brain areas within the same hemisphere remained anatomically intact (scale bar =2 mm).
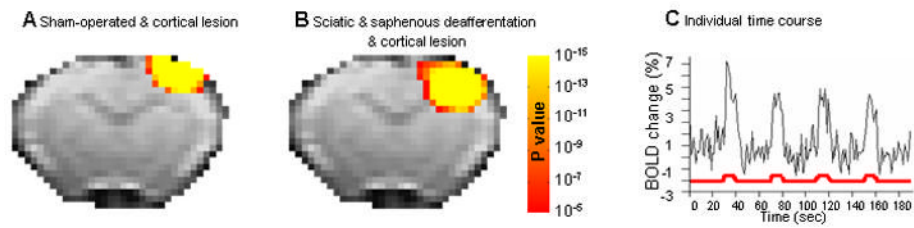
Figure 7.
The effect of somatosensory hindpaw cortical representation lesions on adjacent forepaw cortical activation. Following cortical ablation of the right hindpaw representation, the right forepaw cortical activation, which is adjacent to the hindpaw representation was tested, in order to rule out any damage to other modalities. Following left forepaw stimulation, group t-test map overlaid on a the EPI template image were generated for (A) Sham-operated and cortical lesion and (B) the sciatic and saphenous nerves deafferentation and cortical lesion groups. In addition, a representative BOLD time course taken from the forepaw representation adjacent to the cortical lesion in the saphenous nerves deafferentation and cortical lesion rat is demonstrated (C).
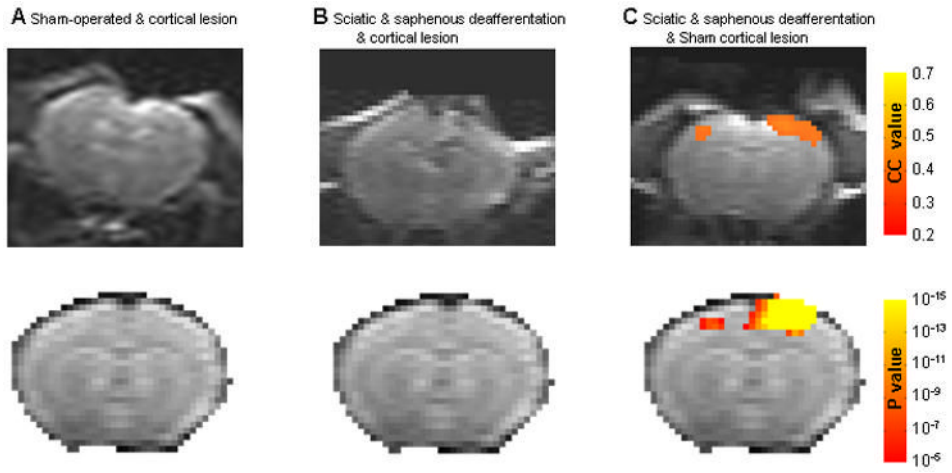
Figure 8.
Representative activation maps and t-test group maps of the hindpaw cortical representation following cortical SI lesion. Upper row: Representative activation maps calculated from cross correlation of p>0.25 overlaid on the original EPI images from three individual rats after intact hindpaw stimulation, from each of the groups (A) Sham-operated with cortical lesion rats, (B) Sciatic and saphenous nerve deffaretiated rats with cortical lesions and (C) Sciatic and saphenous nerves deafferentation with sham-cortical lesions. All SI ablation were positioned in the hindpaw representation contralateral to the healthy hindpaw. In addition, the group t-test maps (p<10^{-5}, corrected for multiple comparison) overlaid on the EPI template image for each of the above groups is displayed in the lower row.

Table 1

Average number of pixels following intact forepaw/hindpaw stimulation in the different groups (mean ± mean standard error).

Forepaw Nerves Deafferentation	**Radial deafferentation n=4**	**Radial & median deafferentation n=4**	**Radial, median & ulnar deafferentation n=4**
Pixel number			
Right somatosensory cortex	47 ± 13	47 ± 4	33 ± 4
Left somatosensory cortex	0 ± 0	0 ± 0	7 ± 1
Hindpaw Nerves Deafferentation	**Sham-operated n=6**	**Sciatic deafferentation n=5**	**Sciatic & saphenous deafferentation n=8**
Pixel number			
Right somatosensory cortex	16 ± 3	8 ± 2	27 ± 5
Left somatosensory cortex	0 ± 0	0 ± 0	14 ± 4